Microelectronic Engineering 179 (2017) 13–17

Contents lists available at ScienceDirect

Microelectronic Engineering

journal homepage: www.elsevier.com/locate/mee

Research paper

Strategy and mechanics for bendable micro-light emitting diode array integrated by polymer

Shiwei Fang [a,b], Jingqiu Liang [a], Zhongzhu Liang [a,*], Yuxin Qin [a], Jinguang Lv [a], Weibiao Wang [a]

[a] The State Key Laboratory of Applied Optics, Changchun Institute of Optics, Fine Mechanics and Physics, Chinese Academy of Sciences, Changchun, Jilin 130033, China
[b] University of Chinese Academy of Sciences, Beijing 100049, China

ARTICLE INFO

Article history:
Received 22 July 2016
Received in revised form 25 March 2017
Accepted 15 April 2017
Available online 18 April 2017

Keywords:
Bendable LED arrays
Mechanical properties
Finite element method
Reliability

ABSTRACT

The strategy for fabricating bendable micro-light emitting diode arrays is presented and the mechanical properties of bent arrays are analysed in this paper. The key procedures of the fabrication process consist of grooving the wafer, welding the upside electrode with an indium tin oxide current-spreading layer, integrating the micro-pixels, removing the substrate, electroplating the backside electrode, and encapsulating the device. In order to prevent potential physical destruction and improve the reliability and fatigue of the arrays, the position of the neutral mechanical plane was calculated. Strain and stress distributions in bent LED arrays showed that strain concentrated in the polymers and the generated stress preferentially concentrated in the electrodes and semiconductor. These results indicate that physical destruction, rupture, or delamination may first occur in the electrodes or semiconductor interface.

1. Introduction

Light emitting diodes (LEDs) have certain advantages, such as high photoelectric transformation efficiency, long lifetime, low energy consumption, and fast response. It has been widely applied in energy-efficient lighting, large screens, backlights of liquid crystal displays, and other fields [1–3]. Moreover, flexible LEDs with bendable or stretchable advantages are promising in flexible lighting [4], biomedical implants [5], conformable displays, and wearable devices [6]. With the increasing availability of mechanically flexible and conformable optoelectronic devices, flexible inorganic LEDs have garnered much attention and many research results have been reported. In general, the reported strategies for fabricating flexible inorganic LEDs include transfer-printing-based assembly methods to position micro-scale inorganic LED pixels on special substrates [7–9], growing or fabricating inorganic LED nanostructures on flexible substrates [10–12], and bonding LED dies onto target flexible circuitry [13]. As semiconductor epitaxial wafers are commonly grown on thick and rigid substrates, which render them incapable of tolerating exceptional levels of mechanical deformation, epitaxial wafers are divided into micro-pixels, which are then integrated together by polymer to fabricate bendable or stretchable micro-LED arrays. In this paper, a strategy to fabricate bendable micro-LED arrays is presented and their mechanical properties are analysed.

2. Strategy

The AlGaInP quaternary system, which is an attractive material system, owing to its direct energy bandgap in the visible wavelength and its spectrum in the yellow-to-red region [14,15], is chosen as the semiconductor epitaxial material. Its multi-layer structure consists of highly doped p-GaP (100 nm–300 nm), a p-GaP window layer, AlGaInP multiple quantum wells (MQWs), a distributed Bragg reflector layer (DBR) (AlGaAs/AlAs, 0.5 μm) that consists of low- and high-reflectivity layers with the optical thickness of 1/4 of the emission wavelength, and an n-GaAs substrate; a cross-section of the epitaxial structure is shown in Fig.1 (a). The window layer with thickness of 6 μm–12 μm is for enhancing current spreading and increasing lateral emitting. In the double-heterostructure AlGaInP-LED, MQWs are between two $Al_{0.35}Ga_{0.15}In_{0.5}P$ cladding layer with thickness of 120 nm and consists of twelve pairs of 8 nm $Ga_{0.49}In_{0.51}P$ quantum well and 10 nm $Al_{0.25}Ga_{0.25}In_{0.5}P$ barrier. GaAs substrate (approximately 350 μm) is lattice matched to DBR and plays a role of supporting in epitaxial process. In following analysis, GaP layer, MQWs and DBR are regarded as the active layer and have a total thickness of 10 μm approximately. We have designed the configuration of the bendable micro-LED arrays to meet the requirements of integrality and bendability, and a model of a 3 × 3 LED array is presented in Fig.1(c). A cross-section of the LED pixel is shown in Fig. 1(b); from top to bottom, the layers of the model include a polymer coating, infilling in the grooves between the LED pixels, upside electrode with quadrate gap, transparent indium tin oxide (ITO) current-spreading layer, semiconductor epitaxial layer, backside electrode, and polyimide substrate. The LED pixels are integrated by a polymer and transferred

* Corresponding author.
E-mail address: liangzz@ciomp.ac.cn (Z. Liang).

http://dx.doi.org/10.1016/j.mee.2017.04.015
0167-9317/

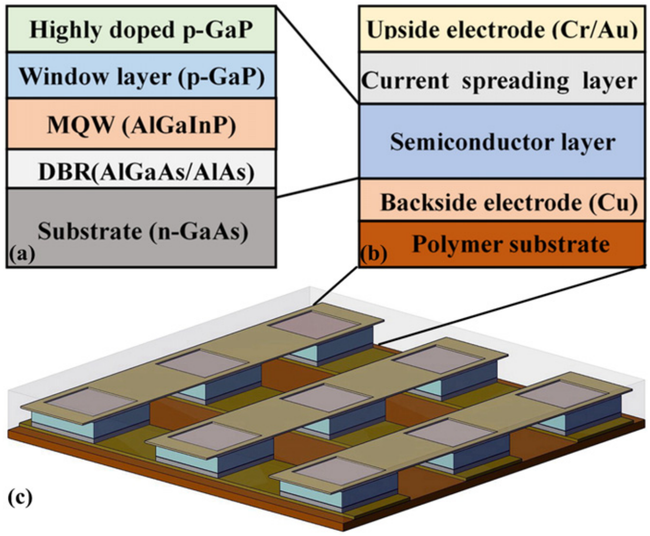

Fig. 1. (a) Cross-section of AlGaInP-LED epitaxial wafer; (b) cross-section of the LED-pixel structure; (c) configuration model of 3 × 3 μ-LED arrays.

onto the target substrate. The polymer Polydimethylsiloxane (PDMS) (Sylgard 184, Dow Corning Corporation, Midland, MI, USA) was chosen for its characteristics of transparency, electrical insulation, hydrophobicity, and high tensile strength. Johnston et al. [16] have shown the variation in the mechanical properties of bulk Sylgard 184 with curing temperature, and the ultimate tensile strength is highest for PDMS test samples cured at 125 °C.

The procedures for fabricating a flexible AlGaInP-LED array are shown in Fig. 2. The intact wafer (Fig. 2(a)) was grooved and divided into square micro-pixels with size of 80 μm × 80 μm. The grooves went through the p-GaP, AlGaInP MQWs, and DBR to the n-GaAs substrate. However, the n-GaAs substrate was still retained as a single unit and the micro-pixels were not entirely separated. As the grooves had a width of 20 μm, the centre distance of two micro-pixels was 100 μm (Fig. 2(b)). In the meantime, a PDMS mould with patterned upside electrodes was fabricated by lithography. The fabrication process of the patterned electrodes consists of forming a plane of PDMS mould on a silicon substrate, patterning and developing the photoresist, depositing metal film, and removing the remaining photoresist. The pattern of the upside electrodes is shown in Fig. 2(i). Then, transparent conductive ITO multilayer electrodes (ITO/Ag/ITO) [17,18] were deposited on the grooved wafer as a current-spreading layer. The multilayer electrodes on grooved wafer were implemented by annealing schemes to improve performance (Fig. 2(c)), and were then welded to the patterned electrodes on the PDMS by cold welding after adjusting the patterns [19] (Fig. 2(d)). However, the welded electrodes were not sufficiently strong to fix the wafer; therefore, the grooves were filled with a liquid PDMS mixture, which was then cured to reinforce the connection. After curing the mixture, LED pixels were integrated together by adhesive PDMS (Fig. 2(e)). Afterwards, the n-GaAs substrate was removed by a chemical process to isolate the LED pixels (Fig. 2(f)). A patterned metal layer was deposited on the backside using lithography and reinforced by electroplating copper (Fig. 2(g)). Finally, the LED array was transferred to a target substrate and encapsulated (Fig. 2(h)). PDMS performs two roles in the strategy to fabricate a bendable micro-LED array; one is to hold the upside electrode and the other is to integrate the LED array. To integrate the LED array, PDMS is used as a bonding material to join isolated LED pixels and to strengthen the electrode connections.

3. Mechanics and experimental results

In a bent array, the internal stress generated by elastic strain impacts the LED-pixels and interconnections. To explore the behaviours of a bent LED array in detail, its mechanical characteristics were analysed by treating a single row of LEDs in the array as a composite beam [20]. For a composite beam with bending deformation, the region adjacent to the neutral mechanical plane (NMP), which defines the position where the strains are zero, exhibits more stable behaviour. Stress and strain are negligible in the regions adjacent to the NMP, such that these sections show more stable and reliable behaviour. The electrodes and active layer (especially the AlGaInP MQWs) play critical roles in the LED array, and their performances and reliability are of primary importance. Therefore, the NMP should be located at the interface between the backside electrodes and the active layer. As a composite beam, the NMP is characterized by the distance d from the top surface, by the following.

$$d = \sum_{i=1}^{N} \overline{E}_i h_i \left(\sum_{j}^{i} h_j - \frac{h_i}{2} \right) \Bigg/ \sum_{i=1}^{N} \overline{E}_i h_i, \quad (1)$$

where N is the total number of layers, hi is the thickness of the ith layer

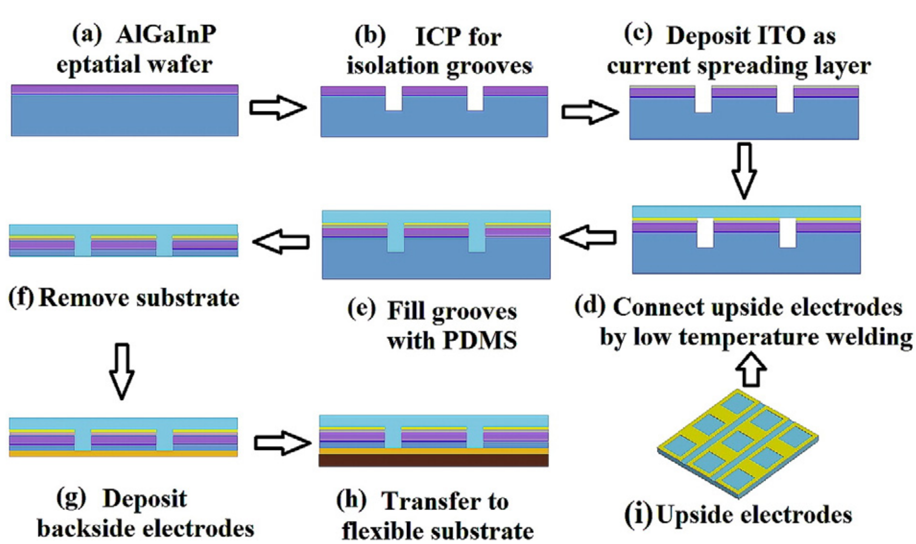

Fig. 2. Procedures for fabricating a bendable AlGaInP-LED array.

(from the top), and

$$\overline{E_i} = E_i/(1-v_i^2). \quad (2)$$

$\overline{E_i}$ is related to the Young's modulus E_i and Poisson's ratio ν_i of the *ith* layer. For the AlGaInP-LED array system, the ultra-thin upside electrode with quadrate gap is neglectful and the LED active layer is regarded as a whole, since the mechanical properties of the semiconductor layers are similar. The elastic properties and layer thicknesses of each layer are as follows. The thicknesses of the PDMS coating and polyimide substrate are variable, the Young's moduli are $E_{PDMS} = 0.0025$GPa and $E_{PI} = 5.1$GPa, and the Poisson's ratios are $\nu_{PDMS} = 0.49$ and $\nu_{PI} = 0.44$. For the ITO current-spreading layer, LED active layer, and backside electrodes, the thicknesses are $h_{ITO} = 0.1$ μm, $h_{LED} = 10$ μm, and $h_{Cu} = 3$ μm, respectively; the Young's moduli are $E_{\mathrm{ITO}} = 118$GPa, $E_{LED} = 85.5$GPa, and $E_{\mathrm{Cu}} = 110$GPa; and the Poisson's ratios are $\nu_{ITO} = 0.3$, $\nu_{LED} = 0.312$, and $\nu_{Cu} = 0.37$. Substituting these data into Eq. (1) and Eq. (2), *d* becomes a function relating the thicknesses of the PDMS coating (h_{PDMS}) and polyimide substrate (h_{PI}). The relationship diagram of the three variables is shown in Fig. 3(a).

However, because the top surface is unfixed and shifts with the PDMS thickness in this model, it is difficult to intuitively obtain information of the position of the NMP. We regarded the top surface of the semiconductor layer (TSS) as a new reference plane to characterize the NMP based on the above results. The distance from the NMP to the TSS is equal to d-h_{PDMS}, expressed as $D = d$-h_{PDMS}. Fig. 3(b) shows the relationship among D, h_{PDMS}, and h_{PI}; D clearly changes with the increasing thickness of the polyimide substrate and the effect of PDMS on D is inconspicuous. In detail, the variation in D with the thickness of the PDMS or polyimide substrate is studied by setting a value for the other thickness. When setting $h_{PI} = 10$ μm, the variation curve of distance D with h_{PDMS} is as shown in Fig. 4(a). Owing to the very small Young's modulus of PDMS compared with the other materials, the distance D slightly decreases (less than 0.01 μm), while h_{PDMS} increases to 60 μm. The change in D, which is a displacement of the NMP upward towards the TSS, is much smaller than the thicknesses of each layer. This demonstrates that the effect of PDMS on the distance D is negligible and the position of the NMP could be treated as immobile. When setting $h_{PDMS} = 10$ μm, the variation of the distance D follows the curve in Fig. 4(b). The position of the NMP moves observably downwards along with the increasing thickness of the polyimide substrate. In particular, to position the NMP at the surface between the backside electrodes and active layer such that $D = 10.1$ μm, the polyimide substrate has a thickness of 44 μm. Generally speaking, the position of the NMP is determined by the thicknesses and mechanical properties of materials and the material with the larger Young's modulus plays a more dominant role.

Based on the above results, we have analysed the mechanical properties of the LED arrays using a finite element method (FEM). In the model, the thicknesses of the PDMS coating and polyimide substrate are 15 μm and 44 μm, respectively. Fig. 5 shows the calculated normal stain and different types of stress distributions in a bent LED array with external pressure. As the existence of active layer makes the stress and strain distributions unsmooth, and the pixel array is periodic and its Young's modulus is high compared to the PDMS filling, the position of

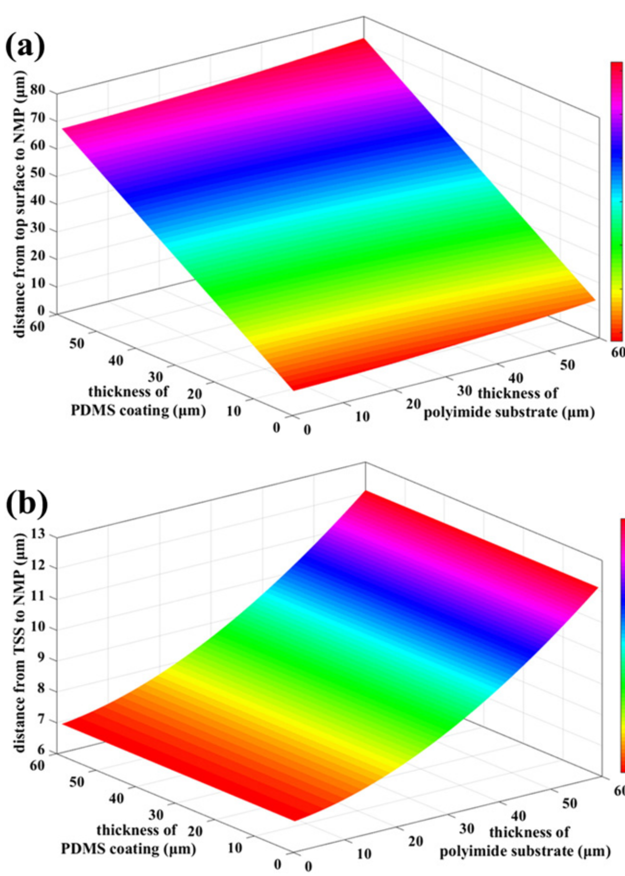

Fig. 3. (a) Relationship diagram of thickness of the PDMS, thickness of the polyimide substrate, and distance from the TSS to NMP; (b) Relationship diagram of thickness of the PDMS, thickness of the polyimide substrate, and distance from the TSS to NMP.

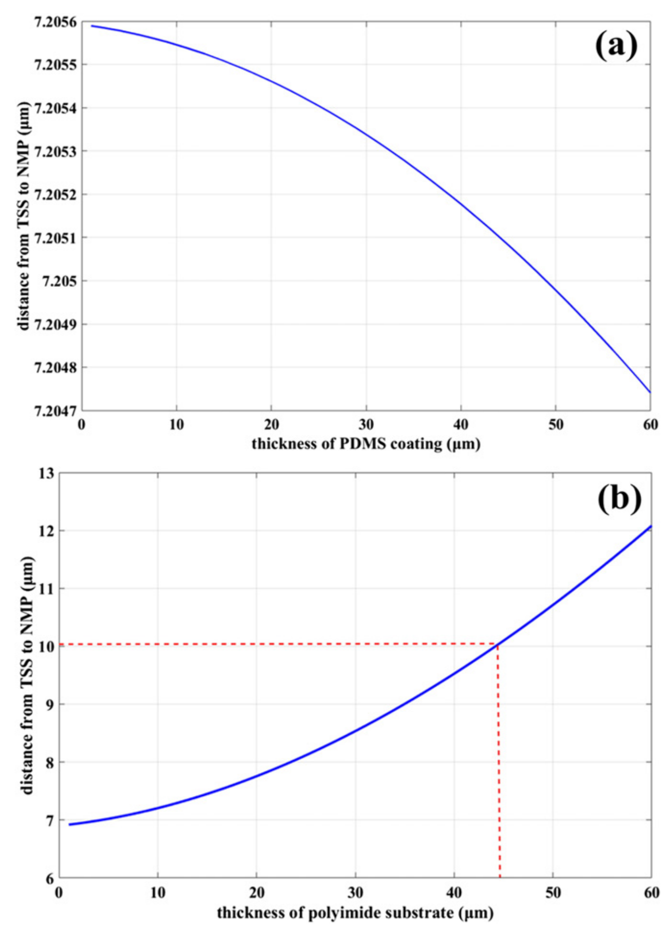

Fig. 4. (a) Variation of the distance from the TSS to NMP with the PDMS as polyimide substrate of 10 μm; (b) variation of the distance from the TSS to NMP with polyimide substrate as PDMS with 10 μm; the intersection of the red dotted line is the point where the NMP is positioned on the interface between the semiconductor and polyimide.

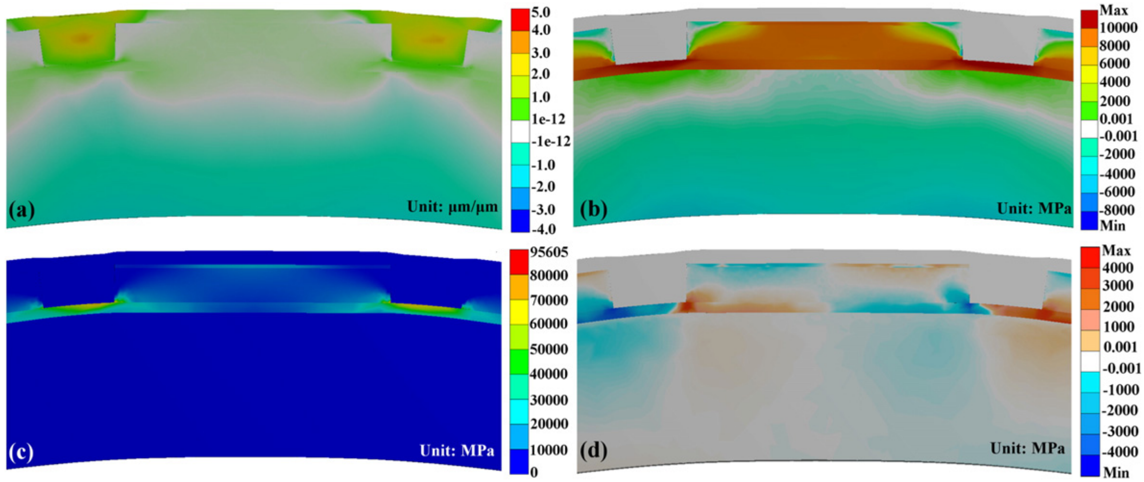

Fig. 5. (a) Elastic stain distribution in bent LED array. Compressive and tensile strain are concentrated in the blue and green regions, respectively, and the tensile stain at the centre of the green regions is higher than at the edges; (b) Elastic stress distribution in bent LED arrays. The red region exhibits high tensile stress and the tensile stress is particularly high in the dark red region. Compressive stress is concentrated in the blue regions; (c) Von Mises stress distribution in bent LED array. The von Mises stress is high in the green regions and it is nearly void in the blue regions; (d) shear stress distribution in bent LED array. The shear stress is concentrated in the red and blue regions, and the acting directions are opposite.

the NMP (white regions in Fig. 5(a)) is not harmonious and regular. The blue and green regions indicate high compressive and tensile strain in Fig. 5 (a), respectively. Owing to the existence of the hard active layer and electrode, the strain is non-uniform in most of the region. The highest strain occurs inside the polymer coating and the substrate, because their Young's moduli are smaller. The strain in the active layer and electrode is relatively low compared to that in other regions. According to the calculated elastic stress distribution shown in Fig. 5(b), there is little stress in the PDMS coating and the high stress is concentrated in the active layer and electrodes with highest Young's moduli among the materials used in the LED array. As a result, potential physical destruction may first occur around the edges of the high-stress regions. There are two kinds of potential physical destruction in a bent LED arrays: rupture and delamination. Fig. 5(c) shows the calculated von Mises stress distribution in the bent LED array. The von Mises stress is a kind of equivalent stress that describes the variation of the inner stress distribution and it could reflect the most dangerous regions in model. Here, the strong von Mises stress present in the electrodes and the strongest is in the copper electrodes between two LED pixels. Therefore, yielding would tend to occur in the copper electrodes between two LED pixels, especially at the pixel edges. This means that plastic deformation or fragmentation may damage these regions earliest if an external pressure is large enough to damage the LED array. On the other hand, the problem of delamination cannot be neglected in a bent LED array, as the elastic strain is inhomogeneous at the interfaces between the electrodes and semiconductor. Fig. 5(c) shows the calculated shear stress distribution in the bent LED array. The shear stress is concentrated in the electrodes at the semiconductor edge, owing to the difference in stiffness between the polymer, metal, and semiconductor. Strong shear stress is observed around the LED pixel edges, as indicated by the deep red and deep blue regions in Fig. 5(d). LED pixel delamination from the copper electrodes is likely to occur in these regions.

In order to test the feasibility of the fabrication strategy and the mechanical properties of the LED array, main procedures were experimentally varied. AlGaInP-LED epitaxial wafer was grooved by inductively coupled plasma etching. The size of each pixel was 80 μm × 80 μm and the width of the grooves was 20 μm. Fig. 6(a) shows a SEM image of grooved wafer in which an array of LED pixels was formed. Then, a liquid PDMS mixture filled in the grooves and coated the upper surface of the LED array under vacuum. After heat-curing the PDMS in a drying oven at 125 °C, the LED array was integrated and ready for removal of the n-GaAs substrate. The GaAs substrate was first etched by a mixture of diluent sulfuric acid and hydrogen peroxide (volume ratio, H_2SO_4:H_2O:H_2O_2 = 1:4:2) to decrease its thickness. Then, a mechanical–chemical method was used to expose the bottom of the PDMS filling, such that LED pixels were totally isolated. An optical image of the isolated micro-LED pixel array is shown in Fig. 6(b), and details of the PDMS filling and adjacent LED pixels are shown in an SEM image in Fig. 6(c). Although the infilling was slightly higher than the surfaces of the pixels, this was acceptable to deposit patterned metal on them. Moreover, the integrated micro-LED pixels were transferred onto polyimide film. The LED array was mechanically flexible and conformable, and the sample could be bent with no observable degradation, even for more than three hundred bending cycles with radius of 10 mm, as shown in Fig. 6(d).

Although the mechanically flexible and conformable LED array sample could bear more than three hundred bending cycles with radius of 50 mm, the capacity to tolerate bending deformation is limited for the LED array. Smaller bending radius means larger stress in the array. As bending radius was 50 mm, the maximum von Mises stress in the array were 62.65 MPa, and that respectively was 308.26 MPa for bending radius of 10 mm and 616.40 MPa for bending radius of 5 mm. Correspondingly, the shear stresses at the semiconductor edge were 0.92 MPa 4.53 MPa, and 9.06 MPa for bending radius of 50 mm, 10 mm, and 5 mm, respectively. Repeated large deformation (i.e. bent with radius of 5 mm) could lead to physical destruction and delamination at the interfaces in the array. There are three ways to take precautions against such damage. The first is to decrease the thickness of the LED pixels, which could enhance the effect of NMP and relieve the concentration of stress and strain. The second is to reduce the LED pixel size and increase the pixel pitch, which could reduce the effect of the LED pixels on the stress (i.e. LED pixel size reduced to 50 μm × 50 μm leads approximately a 10% reduction of maximum von Mises stress as bending radius is 10 mm). The third method is to improve the capacity of electrodes to tolerate stress and deformation by reinforcing the copper electrodes and optimizing the structure.

4. Conclusions

The key procedures of the strategy to fabricate bendable AlGaInP-LED arrays consists of grooving the wafer, welding the upside electrode with an ITO current-spreading layer, integrating the micro-pixels, removing the GaAs substrate, electroplating the backside electrode, and encapsulating the device. In our strategy, the polymer plays two roles

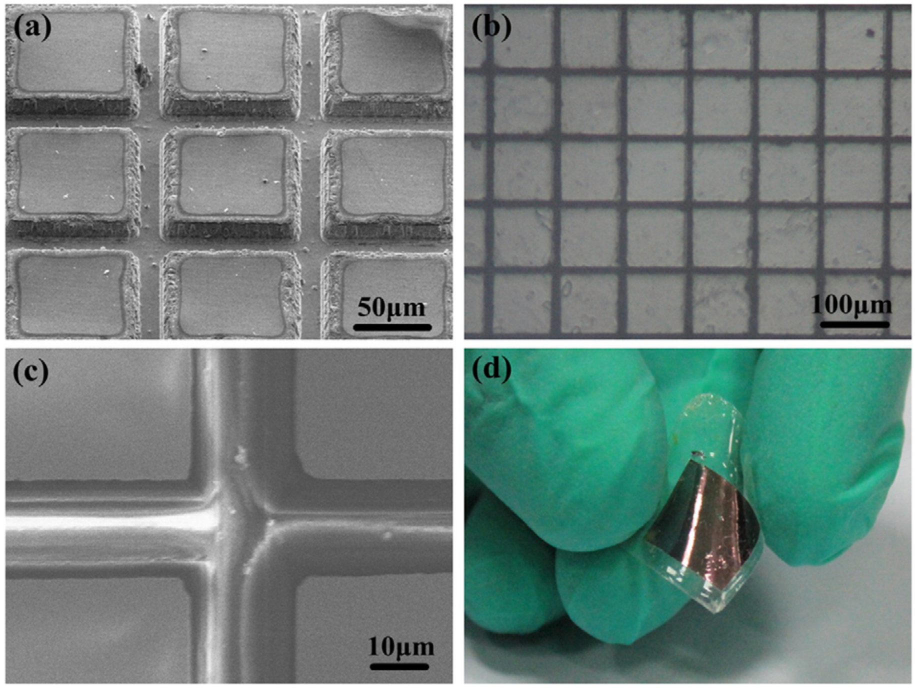

Fig. 6. (a) SEM image of grooved wafer; (b) Optical image of isolated micro-LED pixel array; (c) SEM image of exposed PDMS filling and adjacent LED pixels; (d) Optical image of mechanically flexible and conformable LED array.

in fabricating the bend micro-LED array; one is to hold the electrodes and the other is to integrate LED array. The LED array sample can be bent to radius of 10 mm, with no observable degradation, even for more than three hundred bending cycles. As there is little elastic strain and stress in the region adjacent to the NMP, the structural parameters are optimized to move the NMP to the interface between the backside electrodes and semiconductor layer. We have simulated stress and strain distributions in a bent LED array to study the potential physical destruction. The results show that elastic strain is higher in the polymer layers and elastic stress is concentrated in the semiconductor and electrodes. Moreover, the von Mises stress and shear stress preferentially increase in the electrodes and semiconductor interface, which indicates that these regions are more likely to suffer physical destruction. There are three methods to potentially prevent such destruction, which are decreasing the LED pixel thickness, reinforcing and optimizing the copper electrodes, and finally reducing the LED pixel size and/or increasing the pixel pitch.

Acknowledgments

This work is supported by the National Natural Science Foundation of China (NSFC) under grant 61274122, Jilin Province Science and Technology Development Plan of under grant 20100351, Guangdong Province Science and Technology Plan under grant 2016B010111003.

References

[1] Shang-Ping Ying, Yi-Ching Su, Tien-Li Chang, Chien-PingWang, Microelectron. Eng. 160 (2016) 1–4.
[2] R.D. Dupuis, M.R. Krames, J. Lightwave Technol. 26 (9) (2008) 1154.
[3] Hsiang Chen, Yih-Min Yeh, Chuan Hao Liao, Chun Wei Lin, Chuan-Haur Kao, Tien-Chang Lu, Microelectron. Eng. 101 (2013) 42–46.
[4] H.S. Kim, E. Brueckner, J. Song, Y. Li, S. Kim, C. Lu, J. Sulkin, K. Choquette, Y. Huang, R.G. Nuzzo, J.A. Rogers, Proc. Natl. Acad. Sci. 108 (25) (2011) 10072.
[5] R.H. Kim, D.H. Kim, J. Xiao, B.H. Kim, S.I. Park, B. Panilaitis, R. Ghaffari, J. Yao, M. Li, Z. Liu, V. Malyarchuk, D.G. Kim, A.P. Le, R.G. Nuzzo, D.L. Kaplan, F.G. Omenetto, Y. Huang, Z. Kang, J.A. Rogers, Nat. Mater. 9 (11) (2010) 929.
[6] S.I. Park, Y. Xiong, R.H. Kim, P. Elvikis, M. Meitl, D.H. Kim, J. Wu, J. Yoon, C.J. Yu, Z. Liu, Y. Huang, K.C. Hwang, P. Ferreira, X. Li, K. Choquette, J.A. Rogers, Science 325 (5943) (2009) 977.
[7] R.H. Kim, S. Kim, Y.M. Song, H. Jeong, T.I. Kim, J. Lee, X. Li, K.D. Choquette, J.A. Rogers, Small 8 (20) (2012) 3123.
[8] A.J. Trindade, B. Guilhabert, D. Massoubre, D. Zhu, N. Laurand, E. Gu, I.M. Watson, C.J. Humphreys, M.D. Dawson, Appl. Phys. Lett. 103 (25) (2013) 253302.
[9] Jaeyi Chun, Youngkyu Hwang, Yong-Seok Choi, Jae-Joon Kim, Tak Jeong, Jong Hyeob Baek, Heung Cho Ko, Seong-Ju Park, Scr. Mater. 77 (13) (2014).
[10] J.M. Lee, J.W. Choung, J. Yi, D.H. Lee, M. Samal, D.K. Yi, C.H. Lee, G.C. Yi, U. Paik, J.A. Rogers, W.I. Park, Nano Lett. 10 (8) (2010) 2783.
[11] C.H. Lee, Y.J. Kim, Y.J. Hong, S.R. Jeon, S. Bae, B.H. Hong, G.C. Yi, Adv. Mater. 23 (40) (2011) 4614.
[12] Moon Sung Kang, Chul-Ho Lee, Jun Beom Park, Hyobin Yoo, and Gyu-Chul Yi, Nano Energy 1 (3), 391 (2012).
[13] D.A. van den Ende, R.H.L. Kusters, M. Cauwe, A. van der Waal, J. van den Brand, Microelectron. Reliab. 53 (12) (2013) 1907.
[14] Chao Tian, Weibiao Wang, Jingqiu Liang, Zhongzhu Liang, Yuxin Qin, Jinguang Lv, AIP Adv. 5 (4) (2015) 041309.
[15] Hee Kwan Lee, Myung Sub Kim, Jae Su Yu, Microelectron. Eng. 104 (2013) 29–32.
[16] I.D. Johnston, D.K. McCluskey, C.K.L. Tan, M.C. Tracey, J. Micromech. Microeng. 24 (2014) 035017.
[17] J.H. Lee, K.Y. Woo, K.H. Kim, H.D. Kim, T.G. Kim, Opt. Lett. 38 (23) (2013) 5055.
[18] C. Guillén, J. Herrero, Sol. Energy Mater. Sol. Cells 92 (8) (2008) 938.
[19] Li-Chin Cheng, et al., A high-temperature die-bonding structure fabricated at low temperature for light-emitting diodes, IEEE Electron Device Lett. 36 (2015) 835–837.
[20] S.I. Park, A.P. Le, J. Wu, Y. Huang, X. Li, J.A. Rogers, Adv. Mater. 22 (28) (2010) 3062.